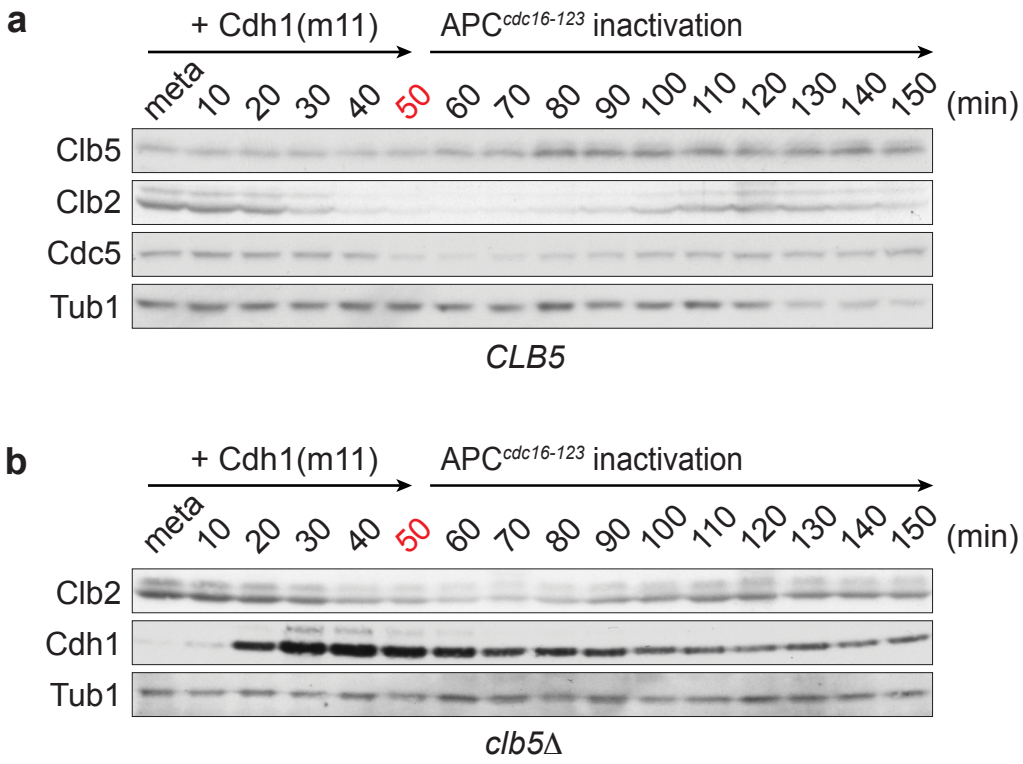

Supplementary Fig. 1 | Comparison of APC targets during Cdh(m11)-induced mitotic exit. **a,** Samples from the Cdh1(m11)-induced reversible mitotic exit experiment in Figure 1 were analysed by Western blotting using antibodies against Clb5, Clb2 and Cdc5. Tub1 served as a loading control. **b,** Reversible Cdh1(m11)-induced Clb2 downregulation in the absence of Clb5. An experiment as in **a** was performed with a strain lacking Clb5.

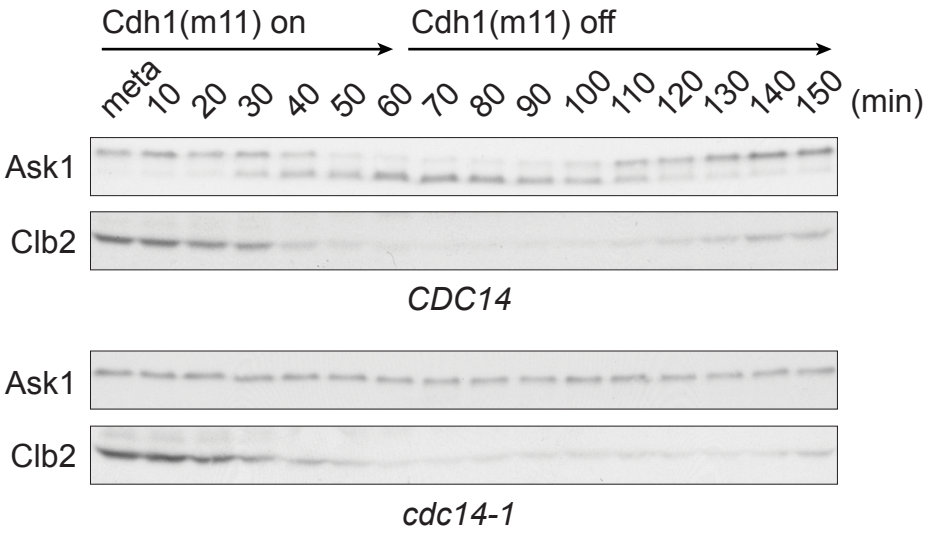

Supplementary Fig. 2 | Ask1 dephosphorylation after Cdh1(m11) expression depends on Cdc14. Cultures of wild type and *cdc14-1* cells were arrested in metaphase by Cdc20 depletion and shifted to 37ºC, a restrictive temperature for the *cdc14-1* allele, 1 hour before induction of Cdh1(m11). After 60 minutes of induction, glucose was added to the culture to terminate Cdh1(m11) expression. Unlike in previous experiments, the APC was not conditionally inactivated during this time course. While Clb2 proteolysis occured similarly in both cultures, Ask1 dephosphorylation was observed in the *CDC14*, but not *cdc14-1*, strain. While the *CDC14* culture completed mitotic exit and entered the next cell cycle (as seen by FACS analysis of DNA content, not shown), *cdc14-1* cells remained arrested in late mitosis.

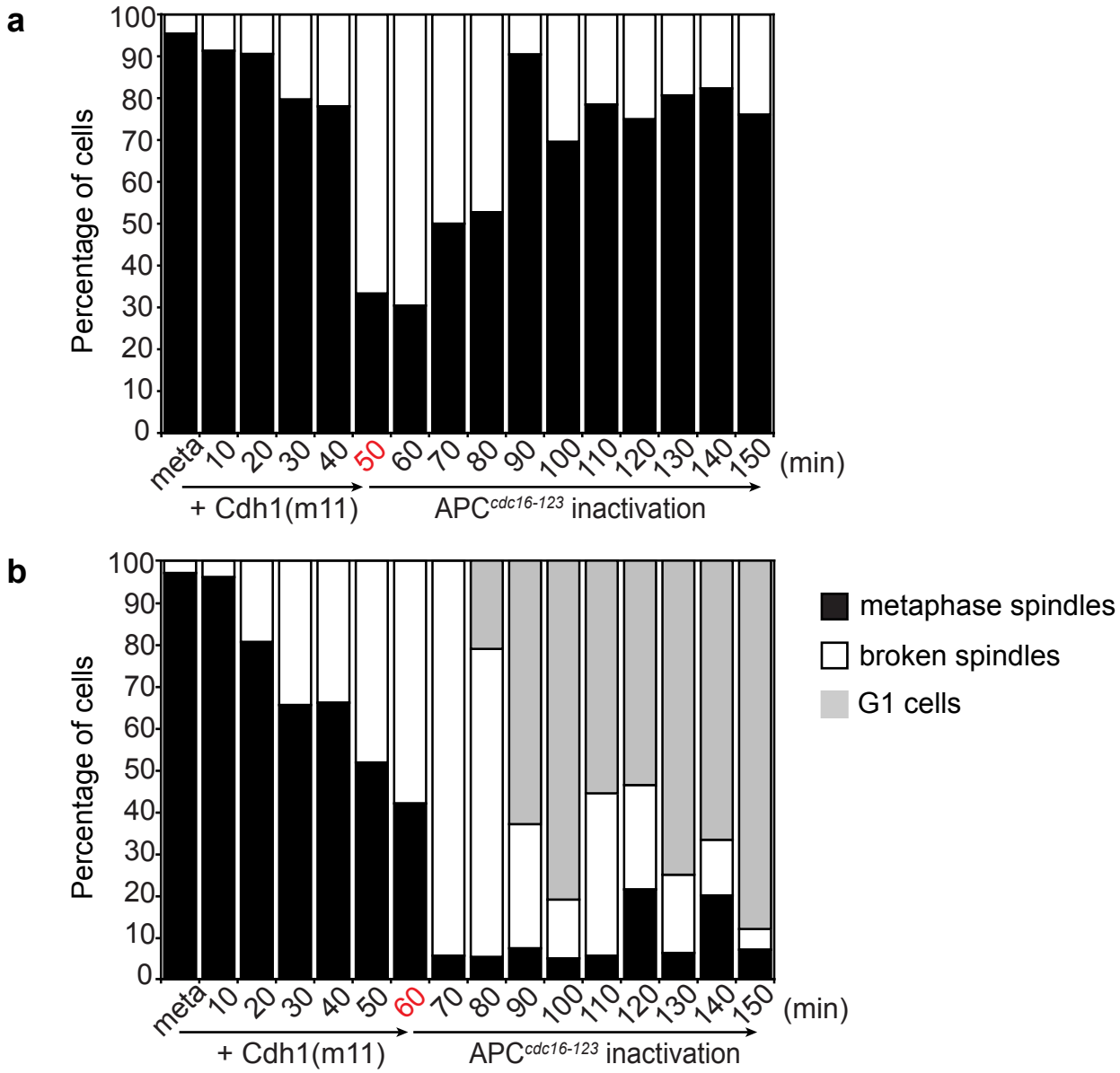

Supplementary Fig. 3 | Quantification of spindle breakdown and re-assembly during reversible and irreversible mitotic exit. Metaphase arrested cells treated **a,** as in Figure 1b (reversible mitotic exit), or **b,** Figure 2a (irreversible mitotic exit), were processed for indirect immunofluorescence to visualise spindles, spindle pole bodies (SPBs) and nuclear DNA, as described in Figure 1c. 30 to 60 cells were scored at every time point and classified according to the presence of an intact metaphase spindle (showing continuous tubulin staining between two separated SPBs), broken spindle (lacking continuous tubulin staining, or collapsed with two adjacent SPBs), or G1 cells containing a single SPB. Whereas spindle disassembly proceeded similarly under both reversible and irreversible conditions, most spindles reassembled when APC$^{cdc16\text{-}123}$ activity was terminated after 50 minutes and Clb2 levels recovered. After 60 minutes, Clb2 no longer recovered, spindles failed to reassemble, and most cells eventually completed mitotic exit and cytokinesis.

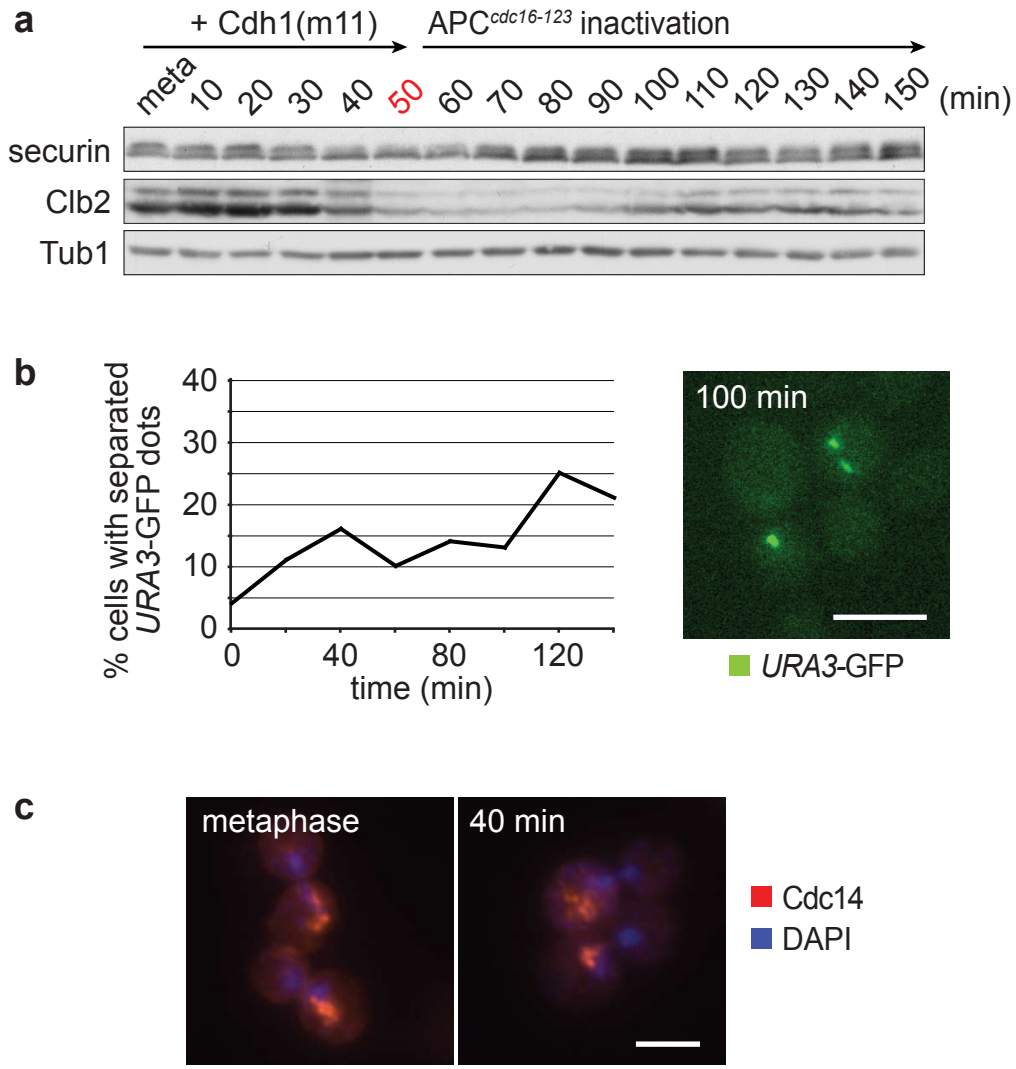

Supplementary Fig. 4 | Inefficient progression of APC^{Cdc20}-dependent anaphase events after Cdh1(m11) expression. a, Destruction of the anaphase inhibitor securin is only inefficiently promoted by Cdh1(m11). Securin levels were analysed by Western blotting during a time course experiment of Cdh1(m11) induction and subsequent *cdc16-123* inactivation, as in Figure 1. While securin was degraded only slowly, we noticed an increase in the faster migrating securin isoform, suggestive of reduced Cdk phosphorylation. Dephosphorylation, in addition to degradation, might weaken separase inhibition by securin[1]. **b,** Slow sister chromatid separation after Cdh1(m11) expression. The status of sister chromatid cohesion was assessed at the GFP-marked *URA3* locus during an experiment similar to the one in **a**. **c,** Cdc14 maintains inhibitory sequestration in the nucleolus after Cdh1(m11) expression. Cells from the experiment in Figure 1 were stained with an affinity-purified α-Cdc14 antibody. Scale bars, 5 μm.

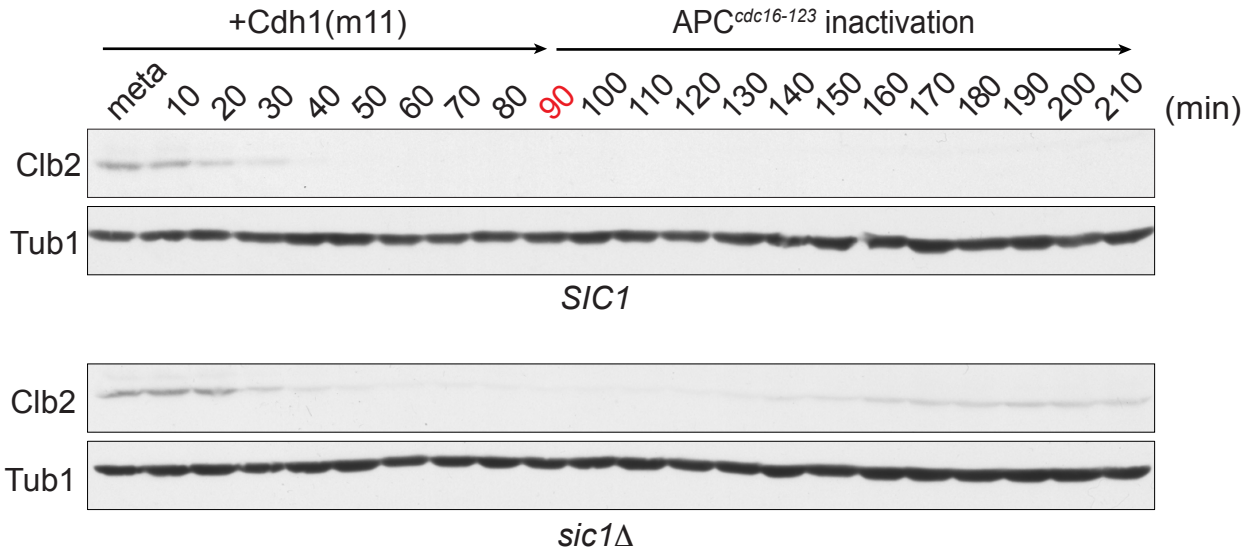

Supplementary Fig. 5 | Sic1 is required for irreversible mitotic exit even after longer periods of Clb2 destruction. Cultures of *SIC1* and *sic1*Δ cells were arrested in metaphase, and Cdh1(m11) was induced as in Figure 2a, but glucose was added to terminate Cdh1(m11) expression and the cultures were shifted to 37ºC to inactivate APC$^{cdc16\text{-}123}$ after 90 min. α-factor (5 μg/ml) was added to prevent progression through the next cell cycle. While Clb2 decreased to almost undetectable levels in both *SIC1* and *sic1*Δ strains, as analysed by Western blotting, APC inactivation resulted in reaccumulation of Clb2 in *sic1*Δ, but not *SIC1*, cells. Tub1 served as a loading control.

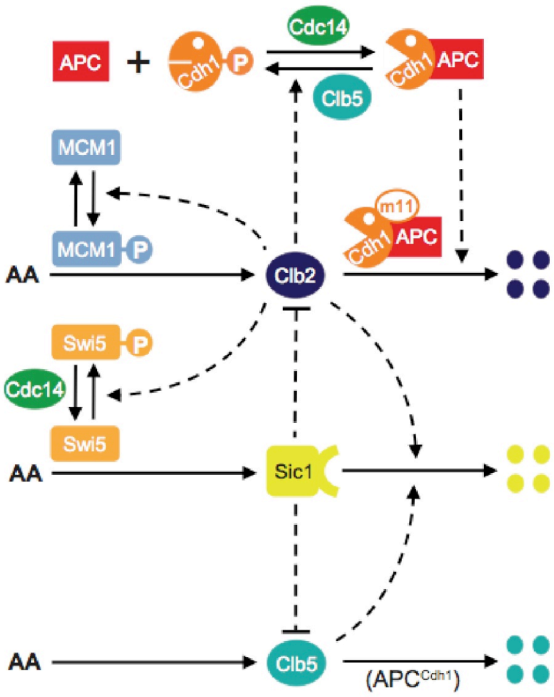

Supplementary Fig. 6 | Mathematical analysis of the irreversibility of mitotic exit in budding yeast. A wiring diagram for regulation of Clb2 kinase and Sic1 in budding yeast is shown[2], used to analyse the relative contributions of proteolysis and feedback loops to the irreversibility of mitotic exit. The wiring diagram from Fig. 4a is redrawn to show details of positive and double-negative feedback loops. Clb2 and Clb5 represent the respective complexes with the Cdk subunit that is neglected from the diagram because it is not rate-limiting. MCM1 represents the Fkh2/Ndd1/Mcm1 transcription factor complex.

The following reactions and interactions were incorporated into this model, based on experimental results in the published literature:

<u>Clb2:</u>
1. Clb2 phosphorylates and activates its own transcription factor Fkh2/Ndd1/Mcm1 by phosphorylation of the Fkh2 and Ndd1 subunits, which creates a positive feedback loop of Clb2 activation[3-5].
2. Unphosphorylated Cdh1 in complex with APC promotes Clb2 ubiquitination and degradation. Clb2 inhibits APC^{Cdh1} activity by phosphorylating Cdh1. This creates a double-negative feedback loop in which reduced Clb2 leads to its increased degradation[6,7]. For simplicity, we have not included endogenous Cdh1 in our model, and it is replaced by constitutively active Cdh1(m11) under inducible control. Inclusion of endogenous Cdh1, which in our experiments is only activated when $APC^{cdc16\text{-}123}$ is already inactive, does not qualitatively influence model behaviour (data not shown).
3. Clb2 kinase activity is further regulated by its stoichiometric inhibitor, Sic1. Clb2 down-regulates Sic1 levels by two mechanisms (see below), creating a pair of double-negative feedback loops that regulate Clb2 activity[8,9].

Swi5/Sic1:
1. Clb2 phosphorylates Swi5, the transcription factor for Sic1. Because phosphorylated Swi5 cannot enter the nucleus, Clb2 inhibits Sic1 synthesis[10]. Swi5 phosphorylation is counteracted by the Cdc14 phosphatase[9].
2. Ubiquitin-mediated Sic1 degradation by the constitutively active SCF ubiquitin ligase depends on Sic1 phosphorylation by Clb2 or Clb5 (ref. 11).

Cdh1:
Clb2 and Clb5 phosphorylate Cdh1, which prevents it from associating with and activating the APC. Reduction of Clb2 and/or Clb5 levels allows the Cdc14 phosphatase to dephosphorylate Cdh1, thereby activating APC^{Cdh1}, creating a double-negative feedback loop that regulates Clb2. A variant of Cdh1 in which 11 Cdk phosphorylation sites have been mutated, Cdh1(m11), activates the APC irrespective of Cdk activity[6,7,9].

Clb5:
Clb5 in this model represents cyclins that activate Cdk in mitosis but that are inefficiently targeted for degradation by Cdh1 (Clb5, Clb6)[12]. However, Clb5 phosphorylates Cdh1 and inhibits APC^{Cdh1} activity[13]. Clb5 is inhibited by Sic1, creating an antagonism between Sic1 and Clb5 (ref. 14). During normal mitotic exit, Clb5 is targeted for degradation by APC^{Cdc20} (ref. 15). As Cdc20 is depleted in our experimental setting, we have to include Clb5 to accurately describe the process. Note, that while removal of Clb5 changes the Sic1 threshold that leads to irreversible mitotic exit, it does not affect the key features of this network. Clb5 was omitted from the analysis of mitotic exit in response to chemical Cdk inhibition.

Cdc14:
Under the experimental conditions used, there was little release of Cdc14 from its inhibition in the nucleolus, which depends on APC^{Cdc20}-dependent securin destruction[16]. We therefore assume a constant, low Cdc14 activity, representing the free form of the phosphatase which is not bound to its inhibitor, Net1 (refs 17,18).

These relationships have been converted into a set of ordinary nonlinear differential equations, which describe the time-rate of change of components on the diagram. All variables are dimensionless and represent relative protein concentrations.

$$\frac{dClb2_T}{dt} = k'_{s,clb2} + k_{s,clb2} \cdot Mcm1P - V_{d,clb2} \cdot Clb2_T$$

$$\frac{dClb5}{dt} = k'_{s,clb5} - V_{d,clb5} \cdot Clb5_T$$

$$\frac{dSic1_T}{dt} = k'_{s,sic1} + k_{s,sic1} \cdot Swi5 - V_{d,sic1} \cdot Sic1_T$$

$$\frac{dTrim2}{dt} = k_{a,s2} \cdot (Clb2_T - Trim2) \cdot (Sic1_T - Trim2 - Trim5) - k_{d,s2} \cdot Trim2 - (V_{d,clb2} + V_{d,sic1}) \cdot Trim2$$

$$\frac{dTrim5}{dt} = k_{a,s5} \cdot (Clb5_T - Trim5) \cdot (Sic1_T - Trim2 - Trim5) - k_{d,s5} \cdot Trim5 - (V_{d,clb5} + V_{d,sic1}) \cdot Trim5$$

$$\frac{dCdh1(m11)}{dt} = k_{s,cdh1} - k_{d,cdh1} \cdot Cdh1(m11)$$

$$\frac{dMcm1P}{dt} = (k'_{a,mcm1} + k_{a,mcm1} \cdot Clb2) \cdot (1 - Mcm1P) - k_{i,mcm1} \cdot Mcm1P$$

$$\frac{dSwi5}{dt} = (k_{a,swi5} + k'_{a,swi5} \cdot Cdc14) \cdot \frac{1 - Swi5}{J_{swi5} + 1 - Swi5} - (k_{i,swi5} + k'_{i,swi5} \cdot Clb2) \cdot \frac{Swi5}{J_{swi5} + Swi5}$$

$$\frac{dInh}{dt} = k_{Inh} \cdot (Inh_o - Inh)$$

$$Clb2 = \frac{Clb2_T - Trim2}{1 + Inh}$$

$$Clb5 = \frac{Clb5_T - Trim5}{1 + Inh}$$

$$V_{d,clb2} = k'_{d,clb2} + k_{d,clb2} \cdot Cdh1(m11) \cdot APC$$

$$V_{d,clb5} = k'_{d,clb5} + k_{d,clb5} \cdot Cdh1(m11) \cdot APC$$

$$V_{d,sic1} = k'_{d,sic1} + k''_{d,sic1} \cdot Clb5 + k_{d,sic1} \cdot Clb2$$

Explanations:

$Clb2_T$ and $Clb5_T$ represent the total concentration of Clb2/Cdk and Clb5/Cdk complexes respectively. Both Clb2/Cdk and Clb5/Cdk can bind reversibly (with dissociation constants of k_d/k_a) to Sic1, forming trimeric complexes (Trim2 and Trim5). We assume that Clb2 and Clb5 kinases are fully inactive in the trimer complexes with Sic1. The level of the active kinases (Clb2 and Clb5) are calculated as difference between the total and the inactive forms ($Clb = Clb_T - Trim$). This is only true, if 1NM-PP1 (Inh) is not present (Inh=0). If 1NM-PP1 is added, it binds rapidly and reversibly to both Cyclin/Cdk dimers and Cyclin/Cdk/Sic1 trimers and the concentration of active complexes is obtained by dividing the concentration of Cyclin/Cdk dimers with (1 + Inh). Inh refers to the intracellular concentration of the inhibitor relative to its IC_{50} value. The inhibitor transport is reversible across the cell membrane with an extracellular concentration of Inh_o. The IC_{50} value for 1NM-PP1 *in vitro* is in the nanomolar range[19], for 5 μM 1NM-PP1 added to the culture medium we estimate $Inh_o = 100$.

The degradation of cyclins (Clb2 and Clb5) and Sic1 was assumed not to be influenced by their complex formation, therefore the same rate constants and rate functions are used to describe the degradation of the different forms.

The total concentration of Swi5 and MCM1 is assumed to be constant (one unit). The differential equations are written on the active forms, which is dephosphorylated in case of Swi5, and the phosphorylated Fkh2/Ndd1/Mcm1 complex (Mcm1P). The level of the inactive

forms is the difference between total and active forms. The interconversions between active and inactive forms of MCM1 are described by mass action, while Michaelis-Menten kinetics is used for Swi5.

APC is assumed to be present in excess and not limiting for complex formation with Cdh1(m11). Therefore APC represents the APC activity rather than its concentration. Its value is one, which is reduced to 0.02 after inactivation of the *cdc16-123* mutant at the restrictive temperature. Cdh1(m11) is synthesized and degraded but not inactivated by Cdk1-dependent phosphorylation. APC binds to Cdh1(m11) and the level of the active complex is the product of Cdh1(m11)·APC.

Only slow synthesis was assumed for Clb5 because its transcription factor (MBF) is inactive during this phase of the cell cycle. Its degradation by APC^{Cdh1} is estimated to be 10-fold slower than Clb2 degradation.

The model was implemented and numerical simulations were performed with the computer programmes WINPP and XPP, using the stiff algorithm. The programmes are freely available from G. Bard Ermentrout (Dept. of Mathematics, Univ. of Pittsburgh, PA, USA, http://www.math.pitt.edu/~bard/xpp/xpponw95.html)

Numerical values of kinetic parameters:
Rate constants (*k's)* have a dimension of min^{-1}, while Michaelis constants are dimensionless.

Clb2 synthesis, degradation and association/dissociation with Sic1:

$k'_{s,clb2} = 0.004$, $k_{s,clb2} = 0.01$, $k'_{d,clb2} = 0.0125$, $k_{d,clb2} = 0.5$, $k_{a,s2} = 10$, $k_{d,s2} = 0.01$

Mcm1 activation/inactivation:

$k'_{a,mcm1} = 0.01$, $k_{a,mcm1} = 2$, $k_{i,mcm1} = 0.2$

Clb5 degradation and association/dissociation with Sic1:

$k_{s,clb5} =$ 0.01 or 0, $k'_{d,clb5} = 0.02$, $k_{d,clb5} = 0.05$, $k_{a,s5} = 10$, $k_{d,s5} = 0.01$

Sic1 synthesis and degradation:

$k'_{s,sic1} = 0.02$, $k_{s,sic1} = 1$, $k_{d,sic1} = 2$, $k'_{d,sic1} = 0.3$, $k''_{d,sic1} = 2$

Swi5 activation/inactivation:

$k_{a,swi5} = 0.01$, $k'_{a,swi5} = 1$, $k_{i,swi5} = 0.01$, $k'_{i,swi5} = 1$, $J_{swi5} = 0.1$

Cdh1(m11) synthesis and degradation:

$k_{s,cdh1} = 0.02$ or 0, $k_{d,cdh1} = 0.02$

Cdc14 and APC:

Cdc14 = 0.02, APC =1 or 0.02

1NM-PP1:

$k_{Inh} = 0.4$, $Inh_o = 100$ or 0

Initial conditions for numerical simulations:
All the simulations were started from a stable steady state representing metaphase arrested cells with high Clb2 and Clb5 kinase activity, low Sic1 levels and inactive Swi5. The initial value of Clb2 is twice that of Clb5, an estimate based on their abundance in asynchronous cultures, and their pattern of accumulation. Clb5 was not included in simulations of mitotic exit in response to 1NM-PP1 addition and APC = 0.02 was used to reflect inactivation of $APC^{cdc16\text{-}1\text{-}23}$. The simulations start with a constant rate of Cdh1(m11) synthesis, or by setting Inh_o from 0 to 100.

$Clb2_T$ = 1.0, Trim2 = 0, Mcm1P = 0.9, $Clb5_T$ = 0.5, Trim5 = 0, Cdh1(m11) = 0, $Sic1_T$ = 0, Swi5 = 0

Supplementary References

1. Agarwal, R. & Cohen-Fix, O. Phosphorylation of the mitotic regulator Pds1/securin by Cdc28 is required for efficient nuclear localization of Esp1/separase. *Genes Dev.* **16**, 1371-1382 (2002).
2. Chen, K. C. *et al.* Integrative analysis of cell cycle control in budding yeast. *Mol. Biol. Cell* **15**, 3841-3862 (2004).
3. Amon, A., Tyers, M., Futcher, B. & Nasmyth, K. Mechanisms that help the yeast cell cycle clock tick: G2 cyclins transcriptionally activate G2 cyclins and repress G1 cyclins. *Cell* **74**, 993-1007 (1993).
4. Reynolds, D. *et al.* Recruitment of Thr 319-phosphorylated Ndd1p to the FHA domain of Fkh2p requires Clb kinase activity: a mechanism for CLB cluster gene activation. *Genes Dev.* **17**, 1789-1802 (2003).
5. Pic-Taylor, A., Darieva, Z., Morgan, B. A. & Sharrocks, A. D. Regulation of cell cycle-specific gene expression through cyclin-dependent kinase-mediated phosphorylation of the forkhead transcription factor Fkh2p. *Mol. Cell. Biol.* **24**, 10036-10046 (2004).
6. Zachariae, W., Schwab, M., Nasmyth, K. & Seufert, W. Control of cyclin ubiquitination by CDK-regulated binding of Hct1 to the anaphase promoting complex. *Science* **282**, 1721-1724 (1998).
7. Jaspersen, S. L., Charles, J. F. & Morgan, D. O. Inhibitory phosphorylation of the APC regulator Hct1 is controlled by the kinase Cdc28 and the phosphatase Cdc14. *Curr. Biol.* **9**, 227-236 (1999).
8. Donovan, J. D., Toyn, J. H., Johnson, A. L. & Johnston, L. H. P40^{SDB25}, a putative CDK inhibitor, has a role in the M/G_1 transition in *Saccharomyces cerevisiae*. *Genes Dev.* **8**, 1640-1653 (1994).
9. Visintin, R. *et al.* The phosphatase Cdc14 triggers mitotic exit by reversal of Cdk-dependent phosphorylation. *Mol. Cell* **2**, 709-718 (1998).
10. Moll, T., Tebb, G., Surana, U., Robitsch, H. & Nasmyth, K. The role of phosphorylation and the CDC28 protein kinase in cell cycle-regulated nuclear import of the S. cerevisiae transcription factor SWI5. *Cell* **66**, 743-758 (1991).
11. Verma, R. *et al.* Phosphoregulation of Sic1p by G_1 Cdk required for its degradation and entry into S phase. *Science* **278**, 455-460 (1997).
12. Schwab, M., Neutzner, M., Möcker, D. & Seufert, W. Yeast Hct1 recognizes the mitotic cyclin Clb2 and other substrates of the ubiquitin ligase APC. *EMBO J.* **20**, 5165-5175 (2001).
13. Yeong, F. M., Lim, H. H., Wang, Y. & Surana, U. Early expressed Clb proteins allow accumulation of mitotic cyclin by inactivating proteolytic machinery during S phase. *Mol. Cell. Biol.* **21**, 5071-5081 (2001).
14. Schwob, E., Böhm, T., Mendenhall, M. D. & Nasmyth, K. The B-type cyclin kinase inhibitor p40^{SIC1} controls the G1 to S transition in *S. cerevisiae*. *Cell* **79**, 233-244 (1994).
15. Shirayama, M., Toth, A., Galova, M. & Nasmyth, K. APC^{Cdc20} promotes exit from mitosis by destroying the anaphase inhibitor Pds1 and cyclin Clb5. *Nature* **402**, 203-207 (1999).
16. Queralt, E., Lehane, C., Novak, B. & Uhlmann, F. Downregulation of PP2A^{Cdc55} phosphatase by separase initiates mitotic exit in budding yeast. *Cell* **125**, 719-732 (2006).
17. Visintin, R., Hwang, E. S. & Amon, A. Cfi1 prevents premature exit from mitosis by anchoring Cdc14 phosphatase in the nucleolus. *Nature* **398**, 818-823 (1999).

18. Shou, W. *et al.* Exit from mitosis is triggered by Tem1-dependent release of the protein phosphatase Cdc14 from nucleolar RENT complex. *Cell* **97**, 233-244 (1999).
19. Bishop, A. C. *et al.* A chemical switch for inhibitor-sensitive alleles of any protein kinase. *Nature* **407**, 395-401 (2000).

Supplementary Table 1: Yeast strains used in this study

(all strains are derivatives of W303)

Figure 1

Y3486 *MATα cdc16-123 MET3-HA-CDC20 GALLp-HA3-CDH1(m11)*

Y3538 as Y3486, *SLI15-Pk$_6$*

Y3508 as Y3486, *ASE1-Pk$_6$*

Y3515 as Y3486, *ASK1-Pk$_6$*

Y3516 as Y3486, *SWI5-myc$_9$*

Figure 2

Y3596 *MATa cdc16-123 MET3-HA-CDC20 GALLp-HA3-CDH1(m11)*

Y3608 as Y3596, *sic1Δ*

Y3516 as above

Y3588 as Y3486, *SIC1-PK$_3$*

Figure 3

Y3596 as above

Y3676 as Y3596, *GAL1-CDC14-myc$_9$*

Y3624 as Y3596, *GAL1-SIC1(m3)-HA*

Y3844 *MATa cdc16-123 MET3-HA-CDC20 GALLp-HA3-CDH1(m11) cdc28-as1 SLI15-Pk$_6$*

Y3852 as 3844, *sic1Δ*

Supplementary Figure 1

Y3508 as above

Y3609 as Y3596, *clb5Δ*

Supplementary Figure 2

Y3636 *MATa MET3-HA-CDC20 GALLp-HA3-CDH1(m11) ASK1-myc$_9$*

Y3635 *MATa cdc14-1 MET3-HA-CDC20 GALLp-HA3-CDH1(m11) ASK1-myc$_9$*

Supplementary Figure 3

Y3596 as above

Supplementary Figure 4

Y3587 as Y3486, *PDS1-myc$_9$*

Y3688 as Y3486, *PDS1-myc$_9$ tetOs::URA3 tetR-GFP*

Y3516 as above

Supplementary Figure 5

Y3596 as above

Y3608 as above